EAI Endorsed Transactions
on Cognitive Communications

Research Article ICST.ORG

# Effective sensor positioning to localize target transmitters in a Cognitive Radio Network

Audri Biswas[1], Sam Reisenfeld[1,*], Mark Hedley, Zhuo Chen[2]

[1]Department of Engineering, Faculty of Science and Engineering, Macquarie University, NSW 2109, Australia
[2]Digital Productivity Flagship, CSIRO, NSW 2122, Australia

## Abstract

A precise positioning of transmitting nodes enhances the performance of Cognitive Radio (CR), by enabling more efficient dynamic allocation of channels and transmit powers for unlicensed users. Most localization techniques rely on random positioning of sensor nodes where, few sensor nodes may have a small separation between adjacent nodes. Closely spaced nodes introduces correlated observations, effecting the performance of Compressive Sensing (CS) algorithm. This paper introduces a novel minimum distance separation aided compressive sensing algorithm (MDACS). The algorithm selectively eliminates Secondary User (SU) power observations from the set of SU receiving terminals such that pairs of the remaining SUs are separated by a minimum geographic distance. We have evaluated the detection of multiple sparse targets locations and error in $l_2$-norm of the recovery vector. The proposed method offers an improvement in detection ratio by 20% while reducing the error in $l_2$-norm by 57%.

Received on 19 June, 2015; accepted on 26 November, 2015; published on 05 April, 2016

**Keywords:** Cognitive Radio, Compressive Sensing, Radio Environment Map, Localization, Power Measurements.



doi:10.4108/eai.5-4-2016.151145

## 1. Introduction

The spectrum scarcity along with inefficient spectrum usage has motivated the development of *Cognitive Radio* (CR). The increasing demand of high data rates due to large numbers of portable hand-held devices initiated significant research in the field of interference mitigation and effective spectral utilization. CR provides a promising solution to the existing problem by efficiently using the underutilized spectrum to facilitate services by *Dynamic Spectrum Sharing* (DSS) for both licensed and unlicensed users. CR technology is based on the concept of learning the state of channel use of *Primary Users* (PUs), and subsequent efficient allocation of channels and transmit parameters to *Secondary Users* (SUs). This allocation takes into account maximum acceptable interference levels to PUs and the throughput and performance requirements of SUs.

In a Cognitive Radio Network, both PUs and SUs share the same channels. Since SUs have lower priority, the channel use is constrained by a maximum acceptable level of interference to PUs. Many efforts have been made in previous literature [1][2] to tackle the issue of interference mitigation but only a few research papers have been published on channel collision avoidance based on the utilization of a *Radio Environment Map* (REM). To generate a REM, the locations of the transmitters and their transmit power levels need to be accurately estimated. From this estimation, the received power level throughout a two dimensional area may be estimated. For the REM, the received power levels interpolated over a two dimensional geographic area are obtained through the use of analytic equations for signal propagation.

In CR, the REM is extremely useful in secondary user channel and transmit parameter selection. This selection must be made with the dual requirements of SU communication effectiveness and bounded interference to PUs. The bounded interference to PUs can only be maintained if the PU locations and received power levels from other PUs, are known by SUs. Therefore an accurate REM is crucial for effective CR operation.

In [3], a cooperative algorithm is formulated that

*Corresponding author. Email: Audri.biswas,Sam.Reisenfeld@mq.edu.au

takes the received signal strength at each SU to create a weighting function and uses it to compute the location of multiple PUs. Although it has relatively low computational complexity, it requires a high density of SUs, and the performance degrades with channel fading. The work in [4] and[5] is based on the concept of using sectorized antennas to detect Direction of Arrival (DOA) of a signal. The phase information of a received signal is exploited to estimate the position of PUs. However, this technique might not be feasible for a practical CRN implementation due to antenna requirements which may be impractical for portable devices.

In this paper we adopt a Compressive Sensing (CS) technique to retrieve the locations of multiple transmitting PUs in a CRN. The approach relies on a location fingerprinting approach, where a certain geographic area is discretised into equally spaced grid points. The PUs are assumed to be positioned at a subset of the grid points. The SUs are also assumed to be positioned at some known locations in the area of interest. Each SU measures Received Signal Strength (RSS) from target PUs. From this set of measurements, there is an attempt to recover the PU locations and transmit power levels. It is usually the case that the number of PUs is much smaller than the number of grid points. Consequently, the set of equations for power levels transmitted by PUs is underdetermined and there are many possible solutions. When the number of PUs is much smaller than the number of grid points, the sparsest solution for the set of equations yields accurate power levels at the correct grid points. Compressive sensing can be used to obtain the data required for the formulation of the REM. Similar techniques were used in [6], [7], [8] and [9].

In a physical system, some of the SUs will be closely geographically located. Having closely placed SUs introduces correlated observations which may increase the observation coherence. Performance of CS algorithms relies heavily on the coherence of the observations from SUs. High coherence among the power measurements makes it difficult for matrix inversion, which may cause inaccurate recovery of the sparse vector. To improve the performance of the CS algorithm, we propose a novel Min-dis-aided CS (MDACS) algorithm. The approach aims to improve the performance of CS algorithms by selectively removing measurements of closely spaced SUs from the set, such as to increase the minimum distance separation between adjacent SUs. The algorithm priorities the RSS of a SU before completely eliminating it from the set. The process generates a refined set of SUs with certain distance separation and high RSS. Our method achieved superior detection of multiple PUs with significantly fewer SU measurements, compared to random deployment of SUs.

In this paper, the locations of SUs are specified by two dimensional vectors. Both the cases of uniform distribution and Gaussian distribution were considered for the random assignment of SU positions. Irrespective of distribution used, our novel approach of pre-selecting SU power measurements appears to achieve reliable detection ratio with fewer receiving nodes. Section II discusses the background of compressive sensing. Sections III-V describe the system model. Section VI-IX presents the simulation results which validate the effectiveness of our proposed method. The conclusion is given in Section VII.

## 2. Compressive Sensing

The CS technique is an approach for the solution of an under-determined set of equations for which the solution vector is known to be sparse. Some data vectors are sparse while others can be made more sparse by an appropriate basis transformation. A typical example would be the time frequency pair. A signal, which is a linear combination of several frequency components, can be easily retrieved by exploiting the sparsity in frequency domain. The complex Fourier Transform basis functions can be used to represent the time domain signal with few non-zero coefficients. In such case the CS algorithm can be used to obtain a sparsest solution vector to a set of underdetermined equations. The sparse vector, $x_{N\times 1}$ is the solution with the minimum number of non-zero elements. If $y_{M\times 1}$ is the raw observation vector obtained by the SU power measurments, there exist the following relationship,

$$y = \phi x, \tag{1}$$

where $\phi_{M\times N}$ is a measurement matrix, representing the power propagation losses from each grid point to each SU. In [7] it states that, a matrix $\phi$ satisfies *Restricted Isometry Property* (RIP) condition, when all subsets of $S$ columns chosen from $\phi$ are nearly orthogonal. Once this is true, there is a high probability of completely recovering the sparse vector with at least $M = CK \times \log_e(N/K)$ measurements (where $K$ is the number of PUs and $C$ is a positive constant) using $l_1$ -minimization algorithm [10]. This can be can be expressed as,

$$min \left\|\vec{x}\right\|_1 = min \sum_i |x_i|$$

subject to

$$\vec{y} = \phi\vec{x}. \tag{2}$$

This formulation is valid for a noiseless scenario but when external noise is considered the algorithm is modified to a *Second-Order Cone Program* for an optimized solution for a defined threshold [10]. This can be stated as,

$$min \left\|\vec{x}\right\|_1 = min \sum_i |x_i|$$

subject to

$$\left\|\vec{y} = \phi\vec{x}\right\|_2 \leq \varepsilon, \tag{3}$$

where $\|\cdot\|_p$ is the $l_p$–norm and $\varepsilon$ is the relaxation constraint for measurement errors. The sparest solution for $\vec{x}$ is the solution with minimum $\|\vec{x}\|_0$. However, the CS algorithm is effective because the same solution vector usually has minimum $l_0$ norm and minimum $l_1$ norm [10].

## 3. System Model

Let us consider a square area discretized into equally spaced $P \times P$ grid where, $K$ PUs are randomly positioned at unique grid points. For simplicity of illustration, we assume that each PU is assigned a single dedicated sub-channel to carry out duplex communication with the base station. Now to observe radio environment and detect the free spectrum, $M$ SUs are deployed randomly in the area of interest. Unlike [6] and [8] the SUs are not placed on the grid points. We adapted a more realistic approach of allowing the SUs to be placed at some known locations in the area. They have the added flexibility of being positioned at non-discretized points on the map. The SUs are controlled and managed by a central node called the *Fusion Centre* (FC). There exist a common control channel between central node and SUs for effective communication of RSS observations and channel allocation information. The FC processes the signal level measurements and manages SU channel allocation. The most crucial assumption in the model is that, spatial coordinates of both the grid points and SUs are known a priori by the FC which receives sensing information from each individual SU. The received power at a SU is a function of distance between the PU and SU as well as shadowing loss. The wireless channels are corrupted by noise and are also considered to be affected by lognormal shadowing. The simplified path-loss model as a function of distance may be described as,

$$Pathloss_{dB}(d) = K_1 + 10\eta log_{10}(\frac{d}{d_0}) + \alpha, \tag{4}$$

where,

- $d$ is transmission distance in meters,
- $d_0$ is the reference distance of the antenna far field,
- $K_1$ is a dimensionless constant in dB,
- $\eta$ is the propagation loss exponent,
- $\alpha$ is the shadowing loss in dB.

$K_1$ is a unit-less constant that relies on the antenna characteristics and average channel attenuation and $K_1 dB = 10log_{10}(K_1)$ [11]. $\alpha$ accounts for the random attenuation of signal strength due to shadowing where $\alpha$ in dB scale is a Gaussian random variable with zero mean and standard deviation $\sigma_{dB} = 5.5$dB [3]. This model was used in [3] for both multipath and shadowing characterization.

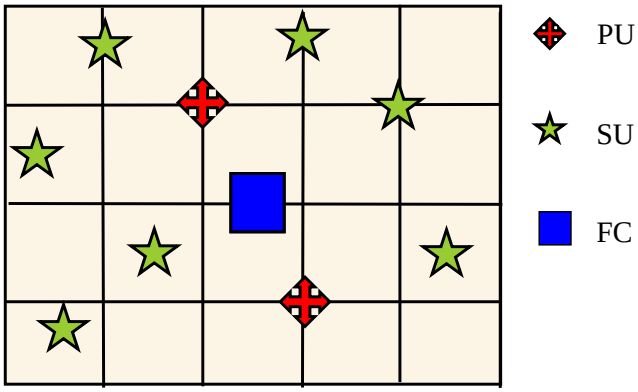


Figure 1. System model demonstrating the positioning of PU, SU and FC

## 4. Localization using compresive sensing

This section combines the location dependent RSS information at each SU to formulate a sparse matrix problem, which can then be solved using the CS method to obtain the exact location of PUs in a CRN. Our grid layout consists of $N$ grid points, with grid resolution $w$ in both x-axis and y-axis. The $N$ grid points are located at $\{V_n, 1 \leq n \leq N\}$, where $V_n$ is a two dimensional position vector. The $M$ SUs are located at $\{U_m, 1 \leq m \leq M\}$, where $U_m$ is also a two dimensional position vector. Earlier in Section III we mentioned $K$ PUs are positioned only at $K$ discrete grids where $K < N$. The FC is assumed to have prior knowledge of $V_n$ and $U_m$. Using the distance information and signal propagation model described in (4) a measurement matrix $\Phi$ is constructed. The entries of the matrix are the channel gain and are expressed using the following equations,

$$d_{mn} = \| U_m - V_n \|_2, \tag{5}$$

$$\Phi_{mn} = 10^{\frac{-Pathloss_{dB}(d_{mn})}{10}}, \tag{6}$$

where $d_{mn}$ is the distance between $m^{th}$ SU and $n^{th}$ grid point and $\Phi_{mn}$ is the pathloss between $m^{th}$ SU and $n^{th}$ grid point. Let Y be a $M \times 1$ column vector where the $m^{th}$ element, $Y_m$, represents the summation of received power from $K$ PUs on $m^{th}$ SU.

$$Y_m = \sum_{k=1}^{K} Q_{m,k}, \tag{7}$$

where,

$$Q_{m,k} = 10^{\frac{Q_{m,k,dB}}{10}}$$

and,

$$Q_{m,k,dB} = P_{k,t} - Pathloss_{dB}(d_{mk})$$

where, $Q_{m,k}$ is the power received at SU $m$ which was transmitted by PU $k$,

$P_{k,t}$ is the power transmitted by user $k$,

and, $d_{m,k}$ is the distance between SU $m$ and PU $k$.

Equation (6) and (7) may be combined to formulate a CS problem similar to (2). It is assumed that the FC has complete knowledge of $\Phi$. Therefore,

$$Y = \Phi X \tag{8}$$

with $X_{N\times 1}$ being a $N \times 1$ column vector, that is to be recovered using CS approach described in Section II. In a realistic scenario, the observations are corrupted with noise power vector $P_n$. The elements of $P_n$ are statistically independent with variance $\sigma_n^2$, and are chi-square distributed with 1 degree of freedom. We can include the effect of additive noise by,

$$Y_n = \Phi X + P_n. \tag{9}$$

Since the model assumes having only few PUs on a large grid size $N$, the vector $X_{N\times 1}$ satisfies the sparsity requirement for accurate recovery using a CS algorithm. Due to its sparse condition, the vector will have only few nonzero elements representing the transmit powers while the indices corresponding to non-zero elements indicate the grid points on which transmitting PUs are located. Hence using a single compressed sensing problem we can jointly estimate both the locations and transmit powers of multiple PUs by solving (3) described in Section II. From the estimation, FS can approximate the received power level throughout a two dimensional area, using the path loss model in (4).

## 5. Data Processing

Based on the problem formulation in Section IV, $Y_{M\times 1}$ is a power observation vector with each row representing sum of RSS received from $K$ PUs on $m^{th}$ SU, and $\Phi_{M\times N}$ is the measurement matrix with channel gain from each grid point. The small grid separation adds large coherence between the columns of the measurement matrix and this may violate the RIP condition[12]. A matrix transformation may be employed to increase the incoherence between the columns. We adopt a data processing technique described in [6] and [8] to decorrelate the rows which are the observation of signal strength from grid points on each SU. Let T be a processing operator,

$$T = SR^{+} \tag{10}$$

where, $S = orth(\Phi^T)^T$. The built in function of Matlab, $orth(B)$ returns an orthonormal basis of the range of $B$, and $B^T$returns the transpose of $B$. $R^+$is the Moore-Penrose pseudoinverse of a matrix $R$, where $R = \Phi$. Applying the operator $T$ on both sides of (9) yields,

$$SR^{+}(Y_n) = SR^{+}\Phi X + SR^{+}P_n = S\Phi^{+}\Phi X + SR^{+}P_n = Ax + \omega$$

$$Y^{'} = AX + \omega. \tag{11}$$

Let $Y^{'}$be $SR^{+}(Y_n)$, the noisy processed observation vector. $A = S\Phi^{+}\Phi$ be the processed measurement matrix and $\omega = SR^{+}P_n$ is the processed measurement noise. The row vectors are being orthogonalised by $S$ while the columns are decorrelated by the influence of $\Phi^{+}\Phi$. Hence we can claim that matrix A satisfies the RIP condition. Note that [6] and [8] considered $\Phi^{+}\Phi = \mathbb{I}_N$, as a diagonal identity matrix. Although $\Phi^{+}\Phi$ acts like an identity on a portion of the space in the sense that it is symmetric. However it is not an identity matrix. After applying the processing operator, CS may be used to recover the sparse vector from processed observation $Y^{'}$, via $l_1$-minimization program [6].

## 6. Simulation And Results

The localization accuracy of the CS algorithm can be effected by certain external factors such as *Signal to Noise Ratio* (SNR), shadowing, density of SUs and distribution of SUs. This section analyses the dependency of these factors on the performance parameters of three $l_1$ constrained optimization algorithms (L1-Magic, OMP and CoSAMP) to produce an accurate result. L1 Magic, CoSAMP, and OMP are three numerical algorithms for constrained $l_1$ vector optimization [13], [14] and [15]. The performance parameters may be categorized as,

$$DetectionRatio = \left[\frac{PU_{Det}}{PU_{Total}}\right]$$

$$Normalized\ Error\ Per\ Grid\ Point = \frac{1}{N}\left\|X_{org} - X_{est}\right\|_2$$

where $PU_{Det}$ is the number of detected PUs; $PU_{Total}$ is the number of the PUs in the network; $X_{org}$ is the original sparse vector; $X_{est}$ the recovered vector using CS algorithms. The average absolute error between the vectors $X_{org}$ and $X_{est}$ is obtained by simulation. This is used to evaluate the accuracy of the algorithms to reconstruct a sparse vector with a minimum number of non-zero coefficients. Furthermore to study the impact of each factor, the simulation is analyzed independently to demonstrate the robustness and reliability of the algorithms.

## 6.1. Simulation Setup

The simulation is carried out on a $43 \times 43$ (i.e. $N = 1849$) square grid with a grid separation of 80m. Among the 1849 grid points, 10 PUs are uniformly distributed on the grid points. The transmit power is random and uniformly distributed over the range of 1 to 5 Watts. The scenario consists of 160 SUs with a two dimensional, zero mean, Gaussian spatial distribution with standard deviation $\sigma_{sd}$. The shadowing factor is log normal distributed.

Simulation (I) - Impact of SNR. Signal to noise ratio is one the crucial factors effecting the performance of each algorithm. SNR is calculated at the receiver as the ratio of average received powers at a SU to $\sigma_n^2$. Where,

$\sigma_n^2$ is the variance of the additive, zero mean, Gaussian nois

Then,

$$SNR(dB) = 10\log_{10}(\frac{1}{M}\sum_{i=1}^{M}\frac{Y_i}{\sigma_n^2}).$$

$Y_i$ is the received RSS from all transmitting PUs at $i^{th}$ SU. As the received signal power is position dependent, SNR will vary with respect to the positioning of SUs. Such scenario prompted us to take the average SNR over $M$ elements of the observation vector. Fig 2(a) and (b) shows the plots for detection ratio of PUs and normalized error per grid versus average received SNR in dB. As shown in Fig.2 (a) when SNR < 12dB, L1-Magic performs better than CoSAMP however when SNR > 15dB, CoSAMP outperforms L1-Magic and OMP. At a higher SNR = 25dB, both CoSAMP and L1-Magic achieved a detection ratio of 1 while OMP is at 0.6. Fig.2(b) shows that, with gradual increase in SNR, CoSAMP generates fewer normalized errors per grid compared to L1-Magic and OMP. Even at a low SNR = 15dB, CoSAMP produces 50% and 54% less errors compared to L1-Magic and OMP.

Similation (II) - Sampling Ratio. Sampling ratio $\frac{M}{N}$ is another major factor that has a significant impact on the performance of these algorithms. In this simulation we start with 200 SUs to detect the position of 10 PUs, where at each iteration 20 SUs are randomly removed to observe the effect of reduced sampling points. The SNR is kept constant at 25dB. The plots in Fig.3 follows a similar trend as in Fig.2. At very low sampling ratio of 0.05, almost all three algorithms fails to recover an accurate sparse solution as solving an undermined system with such small number of measurements is not feasible regardless of any methods used. However with increase in sampling ratio, CoSAMP achieves detection ratio of 1 using 10% less SUs compared to L1-Magic. OMP seems to require higher number of SUs to meet the accuracy of CoSAMP and L1-Magic. Similar conclusion

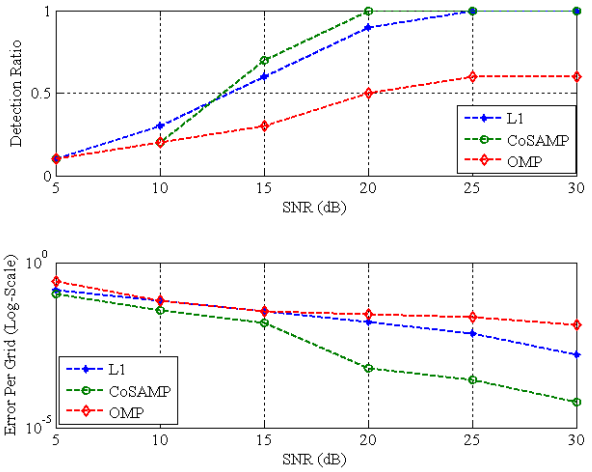


Figure 2. (a) Detection ratio for normal distribution (b) detection ratio for uniform distribution

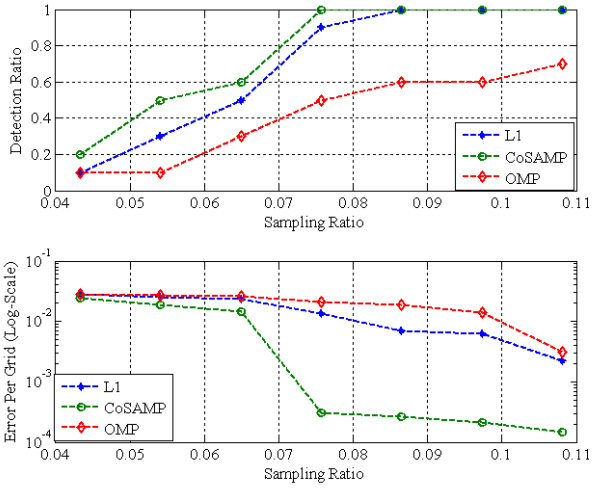


Figure 3. (a) Sampling ratio vs detection ratio (b) sampling ratio vs normalized error per grid

can be drawn from Fig. 3(b), where the graph of normalized error per grid for CoSAMP as a function of sampling ratio decreases much rapidly compared to the other two algorithms. Results from simulation (I) and (II) indicate that, CoSAMP is more robust and can perform with superior results compared to other two algorithms. The next set of simulations will be carried out using CoSAMP and L1-magic only.

## 7. Impactof SU Distribution

In the previous section, the simulations were carried out using SU positions, generated from a two dimensional, zero mean, Gaussian spatial distribution only. This section analyses the influence of the spread

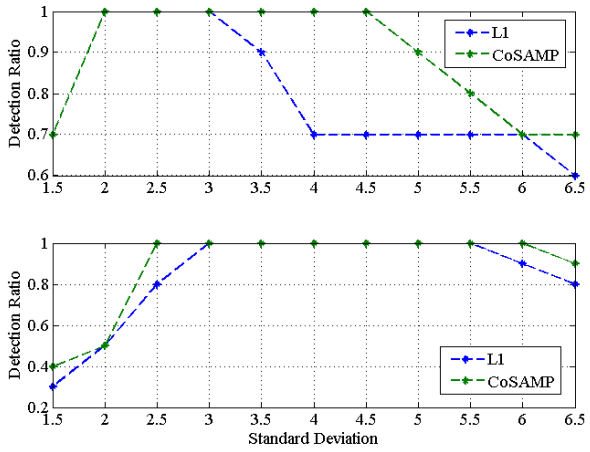


Figure 4. (a) Detection ratio for normal distribution (b) detection ratio for uniform distribution

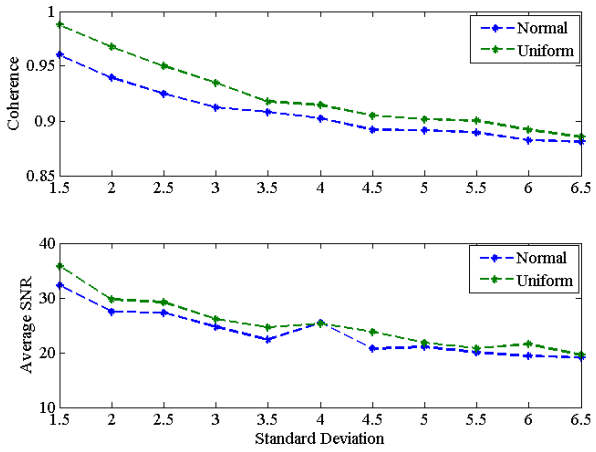


Figure 5. (a) Spread of distribution vs coherence of measurement matrix (b) spread of distribution vs average received SNR.

of a particular spatial distribution, used to obtain location of SUs in a CRN. The two dimensional SU positions are two dimensional random vectors with statistically independent elements. Two cases were considered. In the first case each element is uniformly distributed over $[-X_{max}\sigma_{sd}, X_{max}\sigma_{sd}]$. In the second case, each element is zero mean Gaussian distributed with standard deviation $\{X_{max}\sigma_{sd}\}$. For each of the cases, simulations were carried out with 100 different scenarios. The PU positions are kept constant and the shadowing factor is log normal distributed. The first set of simulations shows the detection ratio of the optimization algorithms, where uniform distribution and Gaussian distribution were considered for the random assignment of SU positions. The second set aims to provide a deeper insight into the effect of the spread of a particular spatial distribution on the coherence of the measurement matrix $\Phi$ and average received SNR at each SU.

While keeping the SNR constant and the number of SUs and PUs constant, the $\sigma_{sd}$ is varied in the range [1.5, 6.5]. Fig. 4 shows the results for the first set of simulations. The figure illustrates the ability to detect the presence of PUs, for a set of SUs drawn from (a) Gaussian normal distribution and (b) uniform distribution respectively. The results are averaged out over 100 scenarios. In Fig 4(a) the SU positions are extracted from a zero mean Gaussian normal distribution. As $\sigma_{sd}$ is varied, the detection ratio increases from 0.7 to 1 and maintains the maximum, until $\sigma_{sd} = 4$ for L1-Magic and $\sigma_{sd} = 5$ for CoSAMP. When $\sigma_{sd} > 5$, the detection ratio has a downward slope irrespective of the algorithms used. And at $\sigma_{sd} = 6.5$ it reaches a minimum point. The set of SUs extracted from a Gaussian normal distribution have a significant proportion of the SUs positioned around the origin. With the spread of the distribution gradually increasing, the SUs are pushed further away from the centre. The sharp tail of Gaussian distribution, extending towards infinity often forces some of the SUs to be positioned at a distance, where channel noise is large with respect to received signal strength. This may cause significant error in the construction of measurement matrix. This may also result in an incorrect recovery of the sparse vector. However due to large distance separation from the transmitting node, the observations at receiving nodes are mutually independent to each other. The independent observations reduces the coherence between the columns of the measurement matrix. Fig. 5(a) clearly shows the gradual reduction in coherence of the measurement matrix for normal distribution with an increase in $\sigma_{sd}$. But in Fig. 5(b) the average received SNR at SUs are also decreasing monotonically while reaching a minimum of less than 20dB. The received SNR is an average value, with some nodes having a received SNR of negative dB or close to 0dB. This explains the behaviour for normal distribution in terms of recovering the sparse vector. In Fig. 4(b), the uniform distribution have a slightly different trend. In case of normal distribution, the algorithms achieved detection ratio of 1 at $\sigma_{sd} = 2$. On the other hand uniform distribution requires $\sigma_{sd} = 2.5$, for at least one of the algorithms to hit a detection ratio of 1. This is solely due to higher coherence between the columns of measurement matrix as shown in Fig. 5(a). In spite of having relatively higher received SNR compared to normal distribution, a large coherence resulted in a poor detection ratio < 0.5. However uniform distribution achieved to maintain the maximum detection ratio for a larger range of $\sigma_{sd}$ [3, 5.5] compared to [2, 3] in case of normal. This is due to

higher received SNR as shown in Fig. 5(b). The working simulations clearly establishes a relationship between the geometry of SU positions and effectiveness of the CS algorithms. The plots also indicates that, with large $\sigma_{sd}$, CS fails to perform efficiently in spite of having lower coherence between the columns of $\Phi$.

## 8. Minimumdistance aided CS algorithm(MDACS)

The following section introduces the Minimum distance aided CS algorithm (MDACS). The proposed modification incorporates received SNR at each individual SUs to deduce the perfect set of measurement nodes. The output of the algorithm is a set of selected SUs, which helps to enhance the performance of CS algorithms. Prior to the improvements, the existing min-dist algorithm [16] relied on selecting a pair of SUs with a specific distance separation between adjacent SUs. The value of separation can be specified by the user. Once the pair is selected, the algorithm randomly removes a SU from the chosen pair. The method iterates through a loop and repeats the procedure until, a refined set is generated such that all SUs are separated from the adjacent SUs by the specified value. With incremental increase in distance separation, the algorithm sequentially eliminates SUs from a given set, until the $l_2$- norm error of the recovered sparse vector is greater than some predefined value. As the previous algorithm depends on random removal of SU nodes, there may be situations where SUs with higher RSS may be accidently eliminated. As a result corrupted measurement data may get included in the observation vector. Such scenarios may restrict CS algorithms from successfully retrieving the sparse vector. Considering the issues with the existing algorithm, the modification uses the RSS at each SU to produce a refined group of SUs with certain geometry. Algorithm 1, provides an informal high-level description of the modified method. The new set of SUs have the required minimum distance separation between each adjacent nodes and high RSS. The separation allows the observation to be independent reducing the coherence in the measurement matrix and high RSS reduces the chance of observations being corrupted by channel noise. Fig. 6 (a) and (b) evaluates the detection ratio of MDACS compared to the existing min-dist algorithm. In Fig. 6(a) the detection ratio has a consistent pattern compared to unusual pattern in Fig. 6(b). The inconsistency is due to random removal of SUs with higher RSS values. Simulation results in Fig. 7(b) shows that, in case of MDACS, the SUs have higher received SNR compared to min-dist. The number of SUs for both the modified and unmodified algorithms are almost identical. Fig. 7(a) indicates that modified algorithm can achieve maximum detection with slightly smaller number of SUs, while maintaining relatively higher SNR.

**Algorithm 1:** Minimum distance aided CS algorithm

**Input:** $\{su\_pos,\ mindist,\ snr\_dB,\ error\}$
**Output:** $Refined\ set\ of\ SU, X_{M\times 1}$
**Method:**

$d \rightarrow mindist$ ;
$snr \rightarrow snr\_dB$ ;
$Q \rightarrow 0$;
$min\_dist \rightarrow min\{pdist(SU\_POS)\}$ ;

**while** (min_dist < d) **do**

**(i)** Find SU pair with separation less than d;
**(ii)** Extract the SU with higher SNR;
**(iii)** Create new set with extracted SUs;
**(iv)** Feed the refined set into CS algorithm;
**(v)** Q = ($l_2$-norm of recovery vector) - Q;

**if** $(Q > error)$, **then**
**break**;
**end**

**end while**

Return $SU\_POS, X_{M\times 1}$

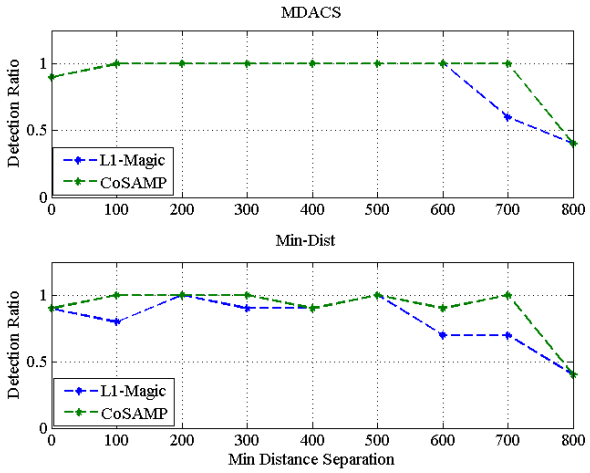


Figure 6. (a) Detection ratio of MDACS (b) detection ratio of existing algorithm.

### 8.1. Simulations

To verify the robustness of our proposed MDACS algorithm, the simulations were carried out for two different sets of distributions. First for Gaussian random distribution and second for uniform random distribution. In the previous section the simulations were conducted only with Gaussian random distribution. In Fig. 8 the effectiveness of our proposed MDACS algorithm is verified in order to successfully detect the presence of PUs

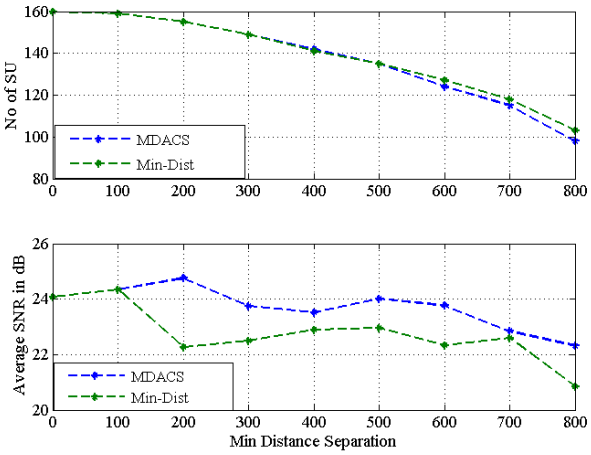


Figure 7. (a) No of SU vs minimum distance separation (b) Average received SNR vs minimum distance separation.

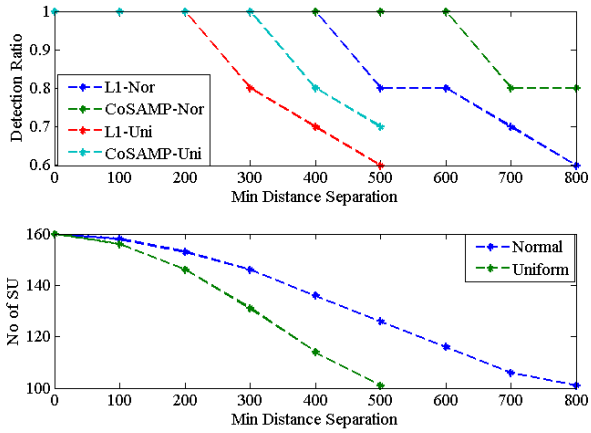


Figure 8. Evaluation of minimum distance algorithm for two different sets of distribution (a) Optimization algorithm for normal distribution (b) optimization algorithm for uniform distribution.

using L1-Magic and CoSAMP algorithms. For each distribution, $\sigma_{sd}$ is kept constant at 2.5. Fig. 8(a), shows the detection ratio plots for each of the MDACS algorithms with respect to the different sets of distributions used for SU positioning. In x axis, we gradually increase the minimum distance separation between the SUs until the detection ratio drops below a certain threshold. Fig. 8(a) shows that for a set of SUs extracted from a uniform distribution, L1-magic and CoSAMP has a detection ratio $< 0.8$, when minimum distance separation is greater than 300m and 400m respectively. A similar trend can be observed in case of normal distribution, where the detection ratio drops below 0.8 at a distance separation of 500m and 700m. From the results, it can be seen that the CS algorithms can maintain a higher detection ratio for a larger distance separation in case of normal compared to uniform. Moreover as shown in Fig. 8(b), with systematic elimination of SUs from a random set, our MDACS algorithm achieved to reduce the number of measurements by 28% for normal distribution and 21% for uniform. In both cases CoSAMP outperformed L1-Magic in terms of achieving higher detection ratio.

## 8.2. Effect on Characteristics of Measurement Matrix

The systematic removal of measurement nodes, impacts the overall structure of the measurement matrix. Fig. 9 gives a deeper insight into the characteristics of each distribution by evaluating parameters, such as coherence of measurement matrix and average received SNR at SUs (observation vector). In previous simulation, with an incremental increase in distance separation, the number of SUs are decreasing. The reduction is due to elimination of SUs by the MDACS algorithm. This has a direct impact on the coherence of the measurement matrix as shown in Fig. 9(a). The measurement matrix is a rectangular matrix, where the

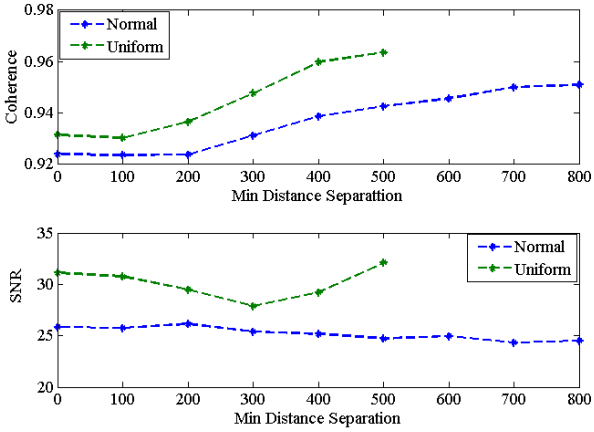


Figure 9. Impact of minimum distance separation on coherence, average received SNR and No of SU.

rows are the observations from each SU. A reduction in number of receiving nodes pushes the coherence of the measurement to a higher value, hence making it difficult for a matrix inversion. For uniform set, the matrix coherence reaches a maximum value of 0.9635 compared to 0.9510 for normal set. According to the theory of CS, a successful recovery of sparse vector is not feasible with matrix having high coherence between the columns. From the working simulations and results, we can clearly conclude that, SU positions extracted from a Gaussian distribution offers better recovery using MDACS algorithm compared to uniform.

## 8.3. Error in Recovery vector

On each iteration of the MDACS algorithm, it removes excess SUs until, the detection ratio or the $l_2$-norm of the recovered sparse vector drops below a certain

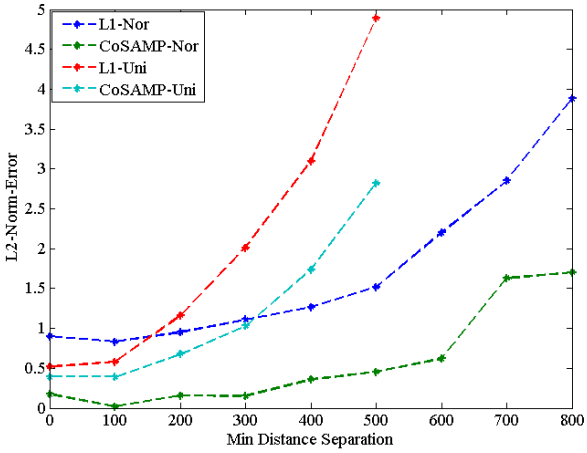


Figure 10. Difference in L2-norm of the recovery vector compared to original vector.

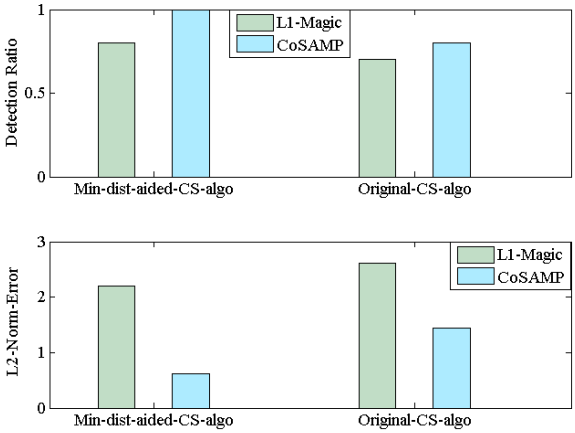


Figure 11. Detection ratio and Error comparison of proposed algorithm compared to original CS algorithm .

threshold. The stopping criteria can be a user defined threshold depending on the application. In scenarios where, localization of nodes have a higher priority, the error threshold can be raised to a higher value. In case of joint localization and exact transmit power reconstruction, error can be restricted to be less than 1. Irrespective of the CS algorithms used, the sparse vector should have the same $l_2 - norm$, as the positioning of PUs and their transmit power level is constant. In Fig. 10, the y-axis represents the difference is $l_2 - norm$ of the recovered vector compared to the original vector. As can be seen in the figure, all the four plots have a similar starting points with slight variations, mainly due to minor errors in accurately determining the transmit powers. Although the plots for uniform distribution have comparative small errors at the start, but with incremental distance separation, there is an exponential increase in the difference in $l_2$-norm. The plot of L1-Uni generates the maximum error with increasing distance separation followed by CoSAMP-Uni, L1-Nor and CoSAMP-Nor. The results indicates that CoSAMP-Nor have the least error while recovering the sparse vector, hence making it suitable for the generation of Radio Environment Map.

## 9. Proposed Algorithm Comparison

The working solutions and results from previous section, concludes that, CoSAMP-MDACS algorithm with SU positions extracted from a Gaussian random distribution generates maximum detection ratio with minimum error. The previous results (Fig. 8) also shows that, during our best case scenario CoSAMP-(MDACS)algorithm achieved a detection ratio of 1, with only 115 SUs. To validate the effectiveness of MDACS algorithm, we compared the performance with original CoSAMP and L1-Magic CS algorithms. In both cases 115 SU positions were extracted from a Gaussian random distribution with $\sigma_{sd} = 2.5$. Fig. 11 illustrates the impact of our proposed method in enhancing the performance of the CS algorithms. Fig. 11(a) shows that, our method allows 20% and 10% more detection for CoSAMP and L1-Magic, compared to the original CS algorithms. Even in case of evaluating the difference in L2-norm-error, Fig. 11(b) indicates that, the proposed technique reduces the error by 57% in CoSAMP and 17% for L1-Magic. Moreover Fig. 12(b), shows that the set of SU generated from the refinement technique have 3% less coherence compared to a randomly deployed set of SUs. Less coherence between the columns allows better structure in the construction of measurement matrix and enables the refined set of SUs to operate at a lower received SNR of 24.95dB compared to 26.73dB as shown in Fig. 12(a).

## 10. Conclusion

The paper discusses the formulation of a novel algorithm to jointly deduce the location and transmit power of PUs in a cognitive radio network. The algorithm exploits the geographic location of the SUs to extract useful information about the positioning of PUs in a network. The proposed method introduces a refinement technique to selectively eliminate closely spaced SUs, in order to reduce the number of correlated observations. The novel method allows each adjacent SUs to have a minimum distance separation, such that the observations at each SUs are nearly independent. Simulation results shows that our novel MDACS algorithm achieved significant improvements in the overall performance of CS algorithms. Simulation results indicate that, our proposed approach has 20% higher detection ratio, while reducing the error by

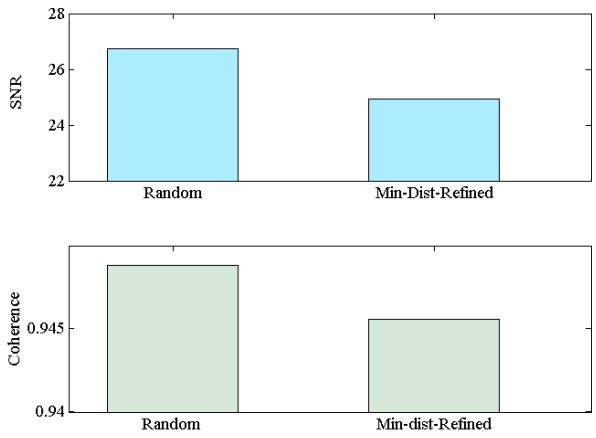


Figure 12. Impact of proposed algorithm on coherence and received SNR at SUs.

57%. Moreover the results also show that our approach generates a set of selective SUs with lower coherence compared to random positioning. This enables CS algorithms to offer perfect recovery at a comparatively lower received SNR. To verify the robustness of the algorithm, we tested our method for two spatial probability distributions for SU positions. In both cases, our algorithm achieved maximum detection ratio with fewer secondary user as receive power sensing. Future work will incorporate the construction of an efficient Radio Environment Map, to detect free spectrum in a geographic area.

## References

[1] S. Wang, Q. Yang, W. Shi, and C. Wang. Interference mitigation and resource allocation in cognitive radio-enabled heterogeneous networks. In *Global Communications Conference (GLOBECOM), 2013 IEEE*, pages 4560–4565, Dec 2013.

[2] D. Hu and S. Mao. Co-channel and adjacent channel interference mitigation in cognitive radio networks. In *Military Communications Conference, 2011 - MILCOM 2011*, pages 13–18, Nov 2011.

[3] A. Mariani, S. Kandeepan, A. Giorgetti, and M. Chiani. Cooperative weighted centroid localization for cognitive radio networks. In *Communications and Information Technologies (ISCIT), 2012 International Symposium on Communication*, pages 459–464, Oct 2012.

[4] J. Werner, J. Wang, A. Hakkarainen, M. Valkama, and D. Cabric. Primary user localization in cognitive radio networks using sectorized antennas. In *Wireless On-demand Network Systems and Services (WONS), 2013 10th Annual Conference on*, pages 155–161, March 2013.

[5] I. Arambasic, J. Q. Casajus, I. Raos, M. Raspopoulos, and S. Stavrou. Anchor-less self-positioning in rectangular room based on sectorized narrowband antennas. In *Wireless Conference (EW), Proceedings of the 2013 19th European*, pages 1–6, April 2013.

[6] C. Feng, S. Valaee, and Z. Tan. Multiple target localization using compressive sensing. In *Global Telecommunications Conference, 2009. GLOBECOM 2009. IEEE*, pages 1–6, Nov 2009.

[7] X. Li, S. Hong, Z. Han, and Z. Wu. Bayesian compressed sensing based dynamic joint spectrum sensing and primary user localization for dynamic spectrum access. In *Global Telecommunications Conference (GLOBECOM 2011), 2011 IEEE*, pages 1–5, Dec 2011.

[8] B.A. Jayawickrama, E. Dutkiewicz, I. Oppermann, G. Fang, and J. Ding. Improved performance of spectrum cartography based on compressive sensing in cognitive radio networks. In *Communications (ICC), 2013 IEEE International Conference on*, pages 5657–5661, June 2013.

[9] H. Jamali-Rad, H. Ramezani, and G. Leus. Sparse multi-target localization using cooperative access points. In *Sensor Array and Multichannel Signal Processing Workshop (SAM), 2012 IEEE 7th*, pages 353–356, June 2012.

[10] E.J. Candes and M.B. Wakin. An introduction to compressive sampling. *Signal Processing Magazine, IEEE*, 25(2):21–30, March 2008.

[11] A. Goldsmith. *Wireless Communications*. Cambridge University Press, New York, NY, USA, 2005.

[12] S. Foucart and H. Rauhut. *A mathematical introduction to compressive sensing*. Springer, 2013.

[13] E.J. Candes and J. Romberg. l1-magic: Recovery of sparse signals via convex programming. *URL: www. acm. caltech. edu/l1magic/downloads/l1magic. pdf*, 4:14, 2005.

[14] J.A. Tropp and A.C. Gilbert. Signal recovery from random measurements via orthogonal matching pursuit. *Information Theory, IEEE Transactions on*, 53(12):4655–4666, Dec 2007.

[15] D. Needell and J. A. Tropp. Cosamp: Iterative signal recovery from incomplete and inaccurate samples. *Applied and Computational Harmonic Analysis*, 26(3):301–321, 2009.

[16] A. Biswas, S. Reisenfeld, M. Hedley, Z. Chen, and P Cheng. Localization of primary users by exploiting distance separation between secondary users. In *Cognitive Radio Oriented Wireless Networks - 10th International Conference, CROWNCOM 2015, Doha, Qatar, April 21-23, 2015, Revised Selected Papers*, pages 451–462, 2015.